Synthesis, Characterization, Solid-State Molecular Structures, and Deprotonation Reactions of Cationic Alcohol Complexes of Osmium Nitrosyl Porphyrins

Lin Cheng,[†] Douglas R. Powell,[‡] Masood A. Khan,[†] and George B. Richter-Addo*[,†]

Department of Chemistry and Biochemistry, University of Oklahoma, 620 Parrington Oval, Norman, Oklahoma 73019, and X-ray Structural Laboratory, Department of Chemistry, University of Wisconsin, 1101 University Avenue, Madison, WI 53706

Received July 7, 2000

New alkoxide (OEP)Os(NO)(OR) (OEP = 2,3,7,8,12,13,17,18-octaethylporphyrinato dianion; R = ethyl, isopropyl, hexyl, cyclohexyl) compounds and alcohol $[(OEP)Os(NO)(HOR)]^+$ complexes (R = methyl, ethyl, isopropyl, hexyl, cyclohexyl) have been prepared in high yields and have been fully characterized by IR, ^1H NMR, and UV−vis spectroscopy, and by elemental analyses. The (OEP)Os(NO)(OEt) compound was characterized by single-crystal X-ray crystallography. The cationic aqua and alcohol $[(OEP)Os(NO)(HOR)]^+$ complexes (R = ethyl, isopropyl, hexyl) complexes were also characterized by single-crystal X-ray crystallography, and the latter represent the first osmium alcohol structures to be reported. The electrophilic $[(OEP)Os(NO)]^+$ cation in the $[(OEP)Os(NO)(HOR)]^+$ complexes renders the coordinated alcohol ligands susceptible to deprotonation by pyridine to produce the corresponding alkoxide (OEP)Os(NO)(OR) derivatives. A one-pot reaction sequence for the preparation of new (OEP)Os(NO)(OR) complexes from (OEP)Os(NO)(OEt) was developed, which was based on (i) initial protonation of the ethoxide compound to give $[(OEP)Os(NO)(HOEt)]^+$, (ii) alcohol substitution by ROH to give $[(OEP)Os(NO)(HOR)]^+$, and (iii) deprotonation of the latter by pyridine to give (OEP)Os(NO)(OR).

Metalloporphyrins of the Group 8 metals containing O-bound axial ligands are potential structural models for the heme-containing catalases[1] or the heme d_1 domain of cytochrome cd_1 nitrite reductase from *Paracoccus denitrificans* GB17 (*Thiospaera pantotropha*).[2] These heme-containing biomolecules contain tyrosinate as an axial ligand, and both these heme enzymes are known to react with nitric oxide (NO) to give heme−NO species.[3] We were interested in developing the chemistry of (por)M(NO)(OR) (por = porphyrinato dianion) complexes as part of our ongoing studies of six-coordinate Group 8 nitrosyl-metalloporphyrins containing mutually trans axial ligands.[4] We have reported a few such nitrosyl porphyrin alkoxide complexes of Ru[5−7] and Os.[6,8] We were intrigued to find out that only a very few solid-state X-ray structures of monometallic osmium alkoxide compounds have been reported, and these include the non-porphyrin $(PPh_3)_2(Br)_3Os(OMe)$,[9] $(salen)Os(O^iPr)_2$ (salen = ethylenebis(salicylidineimine) dianion),[10] $(PEt_2Ph)_2(Cl)_2(NO)Os(OCH_2CH_2OMe)$,[11] and $(P^iPr_3)_2(H)_2Os(OCH_2CF_3)_2$,[12] as well as the porphyrin-containing $(TPP)Os(OR)_2$ (R = Et, ^{i}Pr, Ph)[13] and (OEP)Os(NO)(O^{n}Bu).[8,14]

Surprisingly, however, no solid-state X-ray structures of osmium alcohol compounds have been reported, and only one Group 8 nitrosylmetalloporphyrin alcohol complex has been reported, namely $[(TPP)Fe(NO)(HO-i-C_5H_{11})]^+$.[6] We recently showed that alkoxide complexes of the form (por)M(NO)(OR) (M = Ru, Os) are formed from the formal trans addition reactions of alkyl nitrites (RO−N═O) with the precursor (por)M(CO) compounds.[4] We now report the first synthesis, characterization, and X-ray structural analyses of several alcohol complexes of osmium nitrosyl porphyrins, and show that these complexes undergo facile deprotonation by pyridine to give the corresponding alkoxide derivatives.

Experimental Section

General Procedures. All reactions were performed under an atmosphere of prepurified nitrogen (Airgas) using standard Schlenk techniques and/or in an Innovative Technology Labmaster 100 drybox unless stated otherwise. Solvents (CH_2Cl_2, THF, hexane, and heptane) were distilled from CaH_2 under nitrogen just prior to use.

[†] University of Oklahoma.
[‡] University of Wisconsin.

(1) Valentine, J. S. Dioxygen Reactions. In *Bioinorganic Chemistry*; Bertini, I., Gray, H. B., Lippard, S. J., Valentine, J. S., Eds.; University Science Books: Mill Valley, CA, 1994; Chapter 5; pp 295−298 and references therein.
(2) Williams, P. A.; Fulop, V.; Garman, E. F.; Saunders: N. F. W.; Ferguson, S. J.; Hajdu, J. *Nature* **1997**, *389*, 406−412.
(3) Cheng, L.; Richter-Addo, G. B. Binding and Activation of Nitric Oxide by Metalloporphyrins and Heme. In *The Porphyrin Handbook*; Kadish, K. M., Smith, K. M., Guilard, R., Eds.; Academic Press: New York, 2000; Vol. 4 (Biochemistry and Binding: Activation of Small Molecules), pp 219−291.
(4) Richter-Addo, G. B. *Acc. Chem. Res.* **1999**, *32*, 529−536.
(5) Yi, G.-B.; Khan, M. A.; Richter-Addo, G. B. *Chem. Commun.* **1996**, 2045−2046.
(6) Yi, G.-B.; Chen, L.; Khan, M. A.; Richter-Addo, G. B. *Inorg. Chem.* **1997**, *36*, 3876−3885.
(7) Lee, J.; Yi, G.-B.; Khan, M. A.; Richter-Addo, G. B. *Inorg. Chem.* **1999**, *38*, 4578−4584.
(8) Chen, L.; Khan, M. A.; Richter-Addo, G. B. *Inorg. Chem.* **1998**, *37*, 533−540.
(9) Hinckley, C. C.; Ali, I. A.; Robinson, P. D. *Acta Crystallogr.* **1990**, *C46*, 697−699.
(10) Cheng, W.-K.; Wong, K.-Y.; Tong, W.-F.; Lai, T.-F.; Che, C.-M. *J. Chem. Soc., Dalton Trans.* **1992**, 91−96.
(11) Fergusson, J. E.; Robinson, W. T.; Coll, R. K. *Inorg. Chim. Acta* **1991**, *181*, 37−42.
(12) Kuhlman, R.; Streib, W. E.; Huffman, J. C.; Caulton, K. G. *J. Am. Chem. Soc.* **1996**, *118*, 6934−6945.
(13) Che, C.-M.; Huang, J.-S.; Li, Z.-Y.; Poon, C.-K.; Tong, W.-F.; Lai, T.-F.; Cheng, M.-C.; Wang, C.-C.; Wang, Y. *Inorg. Chem.* **1992**, *31*, 5220−5225.
(14) A few bimetallic and trimetallic osmium compounds containing μ-methoxide or μ-ethoxide ligands have been characterized by X-ray crystallography (refs 15−21).

10.1021/ic0007512 CCC: $20.00
Published on Web 12/01/2000

Chemicals. 2,3,7,8,12,13,17,18-octaethylporphyrin ($OEPH_2$) was obtained from Porphyrin Products (Logan, UT) and used as received. (OEP)Os(CO) was prepared by a literature method.[22] Ethyl nitrite (15 wt. % solution in ethanol), tetrafluoroboric acid (54 wt. % solution in diethyl ether), anhydrous pyridine (99.8%), anhydrous methanol (99.8%), anhydrous ethanol (reagent, denatured), anhydrous 2-propanol (99.5%), hexyl alcohol (98%), and cyclohexanol (99%) were purchased from Aldrich Chemical Co. Chloroform−*d* (99.8%) was obtained from Cambridge Isotope Laboratories, subjected to three freeze−pump−thaw cycles, and stored over Linde 4 Å molecular sieves. Elemental analyses were performed by Atlantic Microlab, Norcross, GA.

Instrumentation. Infrared spectra were recorded on a Bio-Rad FT-155 FTIR spectrometer. ^{1}H NMR spectra were obtained on a Varian XL-400 spectrometer, and the signals (in ppm) were referenced to the residual signal of the solvent employed. All couplings are in hertz. ESI mass spectra were obtained on a Micromass Q-TOF mass spectrometer. UV−vis spectra were recorded on a Hewlett-Packard model 8453 diode array instrument.

Preparation of (OEP)Os(NO)(OEt). To a CH_2Cl_2 (150 mL) solution of (OEP)Os(CO) (1.00 g, 1.33 mmol) was added excess ethyl nitrite (25 mL, 15 wt % in ethanol, ca. 40 mmol). The color of the solution changed from pink-red to bright red immediately. The mixture was stirred at room temperature for 2 h. All volatiles were then removed by rotatory evaporation in air. The red residue was dissolved in a minimum amount of CH_2Cl_2 and chromatographed on a silica gel column (2 × 40 cm) prepared in hexane using a CH_2Cl_2/THF (1:1) mixture as eluent. The red band was collected and taken to dryness by rotary evaporation. Recrystallization of the residue from hot ethanol under N_2 gave (OEP)Os(NO)(OEt) as purple-red crystals (0.830 g, 1.04 mmol, 78% yield) which were collected in air. Anal. Calcd for $C_{38}H_{49}N_5O_2Os\cdot H_2O$: C, 55.93; H, 6.30; N, 8.58. Found: C, 55.68; H, 6.09; N, 8.38. IR (CH_2Cl_2, cm^{-1}): υ_{NO} = 1759. IR (KBr, cm^{-1}): υ_{NO} = 1756 s; also 2966 m, 2933 m, 2871 w, 1469 w, 1448 w, 1365 w, 1316 w, 1274 m, 1230 w, 1155 m, 1103 m, 1064 m, 1057 m, 1020 m, 994 m, 963 m, 843 m, 746 w, 584 w. ^{1}H NMR ($CDCl_3$, δ): 10.32 (s, 4H, *meso*−H of OEP), 4.16 (q, J = 8 Hz, 16H, CH_3CH_2 of OEP), 1.99 (t, J = 8 Hz, 24H, CH_3CH_2 of OEP), −2.65 (q, J = 7 Hz, 2H, OCH_2CH_3), −3.11 (t, J = 7 Hz, 3H, OCH_2CH_3). ESI mass spectrum: *m*/*z* 799 [(OEP)Os(NO)(OEt)]$^+$ (8%), 754 [(OEP)Os(NO)]$^+$ (100%). UV−vis spectrum (λ (ϵ, mM^{-1}cm^{-1}), 7.14 × 10^{-6} M in CH_2Cl_2): 341 (40), 417 (101), 533 (19), 567 (30) nm.

Preparation of [(OEP)Os(NO)(HOEt)]BF_4. To a stirred suspension of (OEP)Os(NO)(OEt) (0.020 g, 0.025 mmol) in anhydrous ethanol (8 mL) was added $HBF_4\cdot Et_2O$ (5 drops, 54 wt % diethyl ether solution, ca. 2.3 mmol). A red homogeneous solution formed immediately. The reaction mixture was refluxed for 2 h. After cooling the reaction mixture to room temperature, heptane (8 mL) was added. Slow solvent evaporation in a drybox over a one week period gave purple crystals of [(OEP)Os(NO)(HOEt)]BF_4 (0.020 g, 0.023 mmol, 90% yield). IR (CH_2Cl_2, cm^{-1}): υ_{NO} = 1828. IR (KBr, cm^{-1}): υ_{NO} = 1814 s; also 2966 m, 2934 w, 2873 w, 1466 m, 1454 m, 1382 m, 1275 m, 1156 s, 1084 s br, 1058 s, 1023 s, 996 m, 964 m, 849 m, 746 w, 736 w. ^{1}H NMR ($CDCl_3$, δ): 10.58 (s, 4H, *meso*−H of OEP), 6.51 (br, free ethanol), 4.23 (m, 16H, CH_3CH_2 of OEP), 3.81 (q, free ethanol), 2.02 (t, J = 8 Hz, 24H, CH_3CH_2 of OEP), 1.12 (t, free ethanol), −2.78 (t, J = 6 Hz, 3H, $HOCH_2CH_3$), −2.84 (t, J = 6 Hz, 2H, $HOCH_2CH_3$). ESI mass spectrum: *m*/*z* 800 [(OEP)Os(NO)(HOEt)]$^+$ (2%), 754 [(OEP)Os(NO)]$^+$ (100%). UV−vis spectrum (λ (ϵ, mM^{-1}cm^{-1}), 9.48 × 10^{-6} M in CH_2Cl_2): 347 (57), 362 (58), 419 (71), 538 (15), 577 (22) nm.

Preparation of Other Alcohol Complexes. The syntheses of the other cationic alcohol complexes paralleled that of the ethanol complex described above, but with the desired alcohol used as the solvent instead of ethanol. The following is a representative example.

Preparation of [(OEP)Os(NO)(HOMe)]BF_4. To a suspension of (OEP)Os(NO)(OEt) (0.030 g, 0.038 mmol) in anhydrous methanol (10 mL) was added $HBF_4\cdot Et_2O$ (3 drops, 54 wt % diethyl ether solution, ca. 1.4 mmol). The red reaction mixture was refluxed for 2 h. The crude red product was isolated as above, and recrystallized from CH_2Cl_2/hexane (1:5, 6 mL) by slow solvent evaporation over a 3-day period (0.030 g, 0.034 mmol, 91% yield). Anal. Calcd for $C_{37}H_{48}N_5O_2OsBF_4\cdot 1.2CH_2Cl_2$: C, 47.12; H, 5.22; N, 7.19. Found: C, 46.96; H, 5.36; N, 7.20. IR (CH_2Cl_2, cm^{-1}): υ_{NO} = 1828. IR (KBr, cm^{-1}): υ_{NO} = 1813 s; also 2965 m, 2933 w, 2874 w, 1718 w, 1700 w, 1696 w, 1653 m, 1577 vw, 1559 m, 1540 w, 1507 m, 1472 w, 1457 w, 1380 m br, 1273 m br, 1157 s, 1084 s br, 1056 s br, 1024 s, 996 s, 965 m, 852 m. ^{1}H NMR ($CDCl_3$, δ): 10.61 (s, 4H, *meso*−H of OEP), 4.24 (q, J = 8 Hz, 16H, CH_3CH_2 of OEP), 2.03 (t, J = 8 Hz, 24H, CH_3CH_2 of OEP), −2.82 (s, 3H, $HOCH_3$). ESI mass spectrum: *m*/*z* 786 [(OEP)Os(NO)(HOMe)]$^+$ (20%), 754 [(OEP)Os(NO)]$^+$ (100%). UV−vis spectrum (λ (ϵ, mM^{-1}cm^{-1}), 7.10 × 10^{-6} M in CH_2Cl_2): 345 (51), 362 (49 sh), 418 (65), 538 (14), 575 (19) nm.

[(OEP)Os(NO)(HO^{i}Pr)]BF_4. 96% yield. IR (CH_2Cl_2, cm^{-1}): υ_{NO} = 1828. IR (KBr, cm^{-1}): υ_{NO} = 1814 s; also 2965 m, 2937 w, 2873 w, 1701 w, 1654 w, 1569 w, 1560 w, 1540 w, 1507 w, 1473 m br, 1458 m br, 1380 m br, 1316 w br, 1273 m, 1156 s, 1111 s br, 1085 s br, 1056 s br, 1023 s, 996 s, 964 m, 849 m, 749 w. ^{1}H NMR ($CDCl_3$, δ): 10.59 (s, 4H, *meso*−H of OEP), 4.24 (q, J = 8 Hz, 16H, CH_3CH_2 of OEP), 2.00 (t, J = 8 Hz, 24H, CH_3CH_2 of OEP), −2.74 (d, J = 7 Hz, 6H, $HOCH(CH_3)_2$), −4.18 (m, 1H, $HOCH(CH_3)_2$). ESI mass spectrum: *m*/*z* 814 [(OEP)Os(NO)(HO^{i}Pr)]$^+$ (1%), 754 [(OEP)Os(NO)]$^+$ (100%). UV−vis spectrum (λ (ϵ, mM^{-1}cm^{-1}), 1.00 × 10^{-5} M in CH_2Cl_2): 347 (56), 361 (57), 419 (69), 539 (15), 577 (22) nm.

[(OEP)Os(NO)(HO(CH$_2$)$_5$CH$_3$)]BF_4. 92% yield. Anal. Calcd for $C_{42}H_{58}N_5O_2OsBF_4\cdot HOCH_2(CH_2)_4CH_3$: C, 55.21; H, 6.95; N, 6.71. Found: C, 55.40; H, 6.93; N, 6.94. IR (CH_2Cl_2, cm^{-1}): υ_{NO} = 1828. IR (KBr, cm^{-1}): υ_{NO} = 1816 s; also 2967 s, 2933 m, 2873 m, 1696 vw, 1653 w, 1576 w, 1570 w, 1559 w, 1540 w, 1507 w, 1472 m br, 1454 m br, 1377 m br, 1274 m br, 1156 m, 1113 m, 1085 s br, 1058 s br, 1023 m, 996 m, 965 m, 849 m, 746 w. ^{1}H NMR ($CDCl_3$, δ): 10.58 (s, 4H, *meso*−H of OEP), 4.24 (q, J = 7 Hz, 16H, CH_3CH_2 of OEP), 3.51 (t, free hexanol), 2.03 (t, J = 8 Hz, 24H, CH_3CH_2 of OEP), 1.44 (m, free hexanol), 1.27 (m, free hexanol), 0.84 (t, free hexanol), 0.36 (m, 5H, $HOCH_2(CH_2)_3CH_2CH_3$), −0.36 (m, 2H, $HOCH_2(CH_2)_3CH_2CH_3$), −1.81 (m, 2H, $HOCH_2(CH_2)_3CH_2CH_3$), −2.57 (m, 2H, $HOCH_2(CH_2)_3CH_2CH_3$), −2.96 (t, J = 7 Hz, 2H, $HOCH_2(CH_2)_3CH_2CH_3$). ESI mass spectrum: *m*/*z* 856 [(OEP)Os(NO)(HOhexyl)]$^+$ (10%), 754 [(OEP)Os(NO)]$^+$ (100%). UV−vis spectrum (λ (ϵ, mM^{-1}cm^{-1}), 8.15 × 10^{-6} M in CH_2Cl_2): 343 (53), 364 (47 sh), 418 (84), 535 (17), 569 (23) nm.

[(OEP)Os(NO)(HOC$_6$H$_{11}$−*cyclo*)]BF_4. 92% yield. Anal. Calcd for $C_{42}H_{56}N_5O_2OsBF_4\cdot 0.5HOC_6H_{11}$: C, 54.59; H, 6.31; N, 7.08. Found: C, 54.56; H, 6.61; N, 6.81. IR (CH_2Cl_2, cm^{-1}): υ_{NO} = 1828. IR (KBr, cm^{-1}): υ_{NO} = 1816 s; also 2964 m, 2926 m, 2869 m, 1274 m, 1227 w, 1156 s, 1112 s, 1060 s, 1021 s, 996 s, 964 s, 845 m, 742 m. ^{1}H NMR ($CDCl_3$, δ): 10.58 (s, 4H, *meso*−H of OEP), 4.24 (m, 16H, CH_3CH_2 of OEP), 3.49 (m, free cyclohexanol), 2.00 (t, J = 8 Hz, 24H, CH_3CH_2 of OEP), 1.81 (m, free cyclohexanol), 1.66 (m, free cyclohexanol), 1.20 (m, free cyclohexanol), 0.18 (d, J = 13 Hz, 1H of HOC_6H_{11}), 0.09 (d, J = 13 Hz, 2H of HOC_6H_{11}), −0.67 (m, 1H of HOC_6H_{11}), −1.13 (m, 2H of HOC_6H_{11}), −1.33 (d, J = 8 Hz, 1H, HOC_6H_{11}), −2.25 (m, 2H of HOC_6H_{11}), −3.44 (d, J = 10 Hz, 2H of HOC_6H_{11}), −4.81 (m, 1H of HOC_6H_{11}). ESI mass spectrum: *m*/*z* 854 [(OEP)Os(NO)(HOC_6H_{11})]$^+$ (30%), 754 [(OEP)Os(NO)]$^+$ (100%). UV−vis spectrum (λ (ϵ, mM^{-1}cm^{-1}), 8.00 × 10^{-6} M in CH_2Cl_2): 342 (46), 364 (40 sh), 417 (77), 535 (15), 569 (21) nm.

Preparation of [(OEP)Os(NO)(HOC$_6$H$_4$F)]BF_4. To a suspension of (OEP)Os(NO)(OEt) (0.012 g, 0.015 mmol) in heptane (10 mL) was

(15) Adams, R. D.; Babin, J. E. *Organometallics* **1987**, *6*, 1364−1365.
(16) Adams, R. D.; Pompeo, M. P.; Tanner, J. T. *Organometallics* **1991**, *10*, 1068−1078.
(17) Adams, R. D.; Babin, J. E. *Organometallics* **1988**, *7*, 2300−2306.
(18) Falloon, S. B.; Szafert, S.; Arif, A. M.; Gladysz, J. A. *Chem.−Eur. J.* **1998**, *4*, 1033−1042.
(19) Arnold, J.; Wilkinson, G.; Hussain, B.; Hursthouse, M. B. *Polyhedron* **1989**, *8*, 597−602.
(20) Braga, D.; Sabatino, P.; Johnson, B. F. G.; Lewis, J.; Massey, A. *J. Organomet. Chem.* **1992**, *436*, 73−77.
(21) Allen, V. F.; Mason, R.; Hitchcock, P. B. *J. Organomet. Chem.* **1977**, *140*, 297−307.
(22) Che, C.-M.; Poon, C.-K.; Chung, W.-C.; Gray, H. B. *Inorg. Chem.* **1985**, *24*, 1277−1278.

Table 1. Crystal Data and Structure Refinement

	(OEP)Os(NO)(OEt)	[(OEP)Os(NO)(H_2O)]BF_4·H_2O	{0.856[(OEP)Os(NO)(EtOH)]BF_4/ 0.144[(OEP)Os(NO)(^{i}PrOH)]BF_4}·^{i}PrOH
formula (fw)	$C_{38}H_{49}N_5O_2Os$ (798.02)	$C_{36}H_{48}N_5O_3OsBF_4$ (875.80)	$C_{41.14}H_{58.29}N_5O_3OsBF_4$ (947.97)
T, K	133(2)	133(2)	133(2)
diffractometer	Bruker SMART CCD	Bruker SMART CCD	Bruker SMART CCD
crystal system	triclinic	triclinic	triclinic
space group	$P\bar{1}$	$P\bar{1}$	$P\bar{1}$
unit cell dimensions	a = 8.675(2) Å, α = 85.525(4)°	a = 10.4973(7) Å, α = 99.0862(16)°	a = 10.8792(9) Å, α = 69.531(2)°
	b = 10.159(3) Å, β = 77.724(4)°	b = 10.6931(7) Å, β = 92.3344(18)°	b = 14.8132(12) Å, β = 71.443(2)°
	c = 11.013(3) Å, γ = 65.186(3)°	c = 16.3071(8) Å, γ = 98.4056(12)°	c = 15.0341(13) Å, γ = 71.450(2)°
V, *Z*	860.7(4) Å^3, 1	1784.25(19) Å^3, 2	2092.7(3) Å^3, 2
D(calcd), g/cm^3	1.540	1.630	1.504
Abs coeff, mm^{-1}	3.744	3.638	3.108
wR(F^2 all data)	0.1477	0.1436	0.0889
Final R(*F* obsd. data)	0.0540	0.0547	0.0389

	[(OEP)Os(NO)($HOCH_2CH_3$)]BF_4·ethanol	[(OEP)Os(NO)($HO(CH_2)_5CH_3$)]BF_4
formula (fw)	$C_{40}H_{56}N_5O_3OsBF_4$ (931.91)	$C_{42}H_{58}N_5O_2OsBF_4$ (941.94)
T, K	163(2)	133(2)
diffractometer	Bruker P4	Bruker SMART CCD
Crystal system	triclinic	monoclinic
Space group	$P\bar{1}$	$P2_1$
Unit cell dimensions	a = 10.604(2) Å, α = 69.661(14)°	a = 12.7943(9) Å, α = 90°
	b = 14.867(3) Å, β = 72.42(2)°	b = 22.0541(14) Å, β = 102.796(2)°
	c = 14.949(3) Å, γ = 71.516(12)°	c = 15.1707(8) Å, γ = 90°
V, *Z*	2046.6(7) Å^3, 2	4174.4(5) Å^3, 4
D(calcd), g/cm^3	1.512	1.499
Abs coeff, mm^{-1}	3.176	3.114
wR(F^2 all data)	0.1234	0.0827
Final R(*F* obsd. data)	0.0461	0.0369

added excess solid 4-fluorophenol (0.5 g, 4.5 mmol) and HBF_4·Et_2O (5 drops, 54 wt % diethyl ether solution, ca. 2.4 mmol). The mixture was refluxed for 3 h. After cooling to room temperature, the reaction mixture was filtered to remove unreacted 4-fluorophenol. The filtrate was taken to dryness in vacuo to give [(OEP)Os(NO)(HOC_6H_4F)]BF_4 as a red solid. ^{1}H NMR ($CDCl_3$, δ): 10.55 (s, 4H, *meso*−H of OEP), 4.18 (q, J = 8 Hz, 16H, CH_3CH_2 of OEP), 1.98 (t, J = 7 Hz, 24H, CH_3CH_2 of OEP), 1.22 (m, 2H of HOC_6H_4F), 0.65 (s, 2H of HOC_6H_4F).

Deprotonation of Cationic Alcohol Complexes with Base. The following reaction is representative: To a CH_2Cl_2 (3 mL) solution of [(OEP)Os(NO)(HOMe)]BF_4 (0.008 g, 0.009 mmol) was added excess pyridine (0.3 mL). The red color of the solution immediately turned bright pink-red. After stirring under N_2 in the dark for 5 min, all volatiles were removed in vacuo. The red residue was dissolved in a minimum amount of CH_2Cl_2 and quickly chromatographed on a silica gel column. Elution with a mixture of CH_2Cl_2/THF (5:1) gave the pure known alkoxide compound (OEP)Os(NO)(OMe) (0.005 g, 0.0063 mmol, 70% yield). ^{1}H NMR ($CDCl_3$, δ): 10.44 (s, 4H, *meso*−H of OEP), 4.19 (q, J = 7 Hz, 16H, CH_3CH_2 of OEP), 2.00 (t, J = 7 Hz, 24H, CH_3CH_2 of OEP), −2.82 (s, 3H, OCH_3).

Preparation of Alkoxide Complexes from (OEP)Os(NO)(OEt). The following is representative: To a suspension of (OEP)Os(NO)(OEt) (0.018 g, 0.023 mmol) in 2-propanol (8 mL) was added HBF_4·Et_2O (5 drops, 54 wt % diethyl ether solution, ca. 2.3 mmol) in the dark. The red solution was refluxed for 2 h. All volatiles were removed in vacuo, and the residue was dissolved in CH_2Cl_2 (3 mL) and pyridine (0.5 mL). The solution was stirred at room temperature for 5 min. All volatiles were removed in vacuo. The red residue was dissolved in a minimum amount of CH_2Cl_2 and quickly chromatographed on a short silica gel column by using CH_2Cl_2/THF (5:1) as eluent (the known [(OEP)Os(NO)]$_2$(μ-O)[23] also forms if the alkoxide compound stays in contact with the silica gel column for a longer period). The red band was collected and taken to dryness, and the alkoxide compound (OEP)Os(NO)(O^iPr) was obtained as a red solid (0.012 g, 0.015 mmol, 65% yield). IR (CH_2Cl_2, cm^{-1}): υ_{NO} = 1756. IR (KBr, cm^{-1}): υ_{NO} = 1743 s; also 2964 s, 2932 m, 2869 w, 1468 m, 1373 w, 1272 w, 1230 vw, 1155 m, 1112 w, 1057 m, 1021 m, 993 m, 983 m, 964 m, 843 m, 737 m. ^{1}H NMR ($CDCl_3$, δ): 10.32 (s, 4H, *meso*−H of OEP), 4.16 (q, J = 8 Hz, 16H, CH_3CH_2 of OEP), 1.97 (t, J = 7 Hz, 24H, CH_3CH_2 of OEP), −3.02 (d, J = 6 Hz, 6H, $OCH(CH_3)_2$), −4.17 (m, 1H, $OCH(CH_3)_2$). ESI mass spectrum: m/z 814 [(OEP)Os(NO)(O^iPr)]$^+$ (5%), 754 [(OEP)Os(NO)]$^+$ (100%). UV−vis spectrum (λ (ϵ, mM^{-1}cm^{-1}), 1.06 × 10^{-5} M in CH_2Cl_2): 341 (36), 418 (91), 533 (17), 567 (26) nm.

(OEP)Os(NO)(O(CH$_2$)$_5$CH$_3$). 60−70% yield. IR (CH_2Cl_2, cm^{-1}): υ_{NO} = 1757. IR (KBr, cm^{-1}): υ_{NO} = 1754 s. ^{1}H NMR ($CDCl_3$, δ): 10.32 (s, 4H, *meso*−H of OEP), 4.16 (q, J = 7 Hz, 16H, CH_3CH_2 of OEP), 1.99 (t, J = 8 Hz, 24H, CH_3CH_2 of OEP), 0.37 (m, 5H, $OCH_2(CH_2)_3CH_2CH_3$), −0.29 (m, 2H, $OCH_2(CH_2)_3CH_2CH_3$), −1.63 (m, 2H, $OCH_2(CH_2)_3CH_2CH_3$), −2.80 (t, J = 7 Hz, 2H, $OCH_2(CH_2)_3CH_2CH_3$), −3.03 (s, 2H, $OCH_2(CH_2)_3CH_2CH_3$).

(OEP)Os(NO)(OC$_6$H$_{11}$−*cyclo*). 60−70% yield. IR (CH_2Cl_2, cm^{-1}): υ_{NO} = 1755. IR (KBr, cm^{-1}): υ_{NO} = 1751 s. ^{1}H NMR ($CDCl_3$, δ): 10.32 (s, 4H, *meso*−H of OEP), 4.16 (m, 16H, CH_3CH_2 of OEP), 1.97 (t, J = 8 Hz, 24H, CH_3CH_2 of OEP), with the OC_6H_{11} peaks at 0.16 (d, J = 13 Hz, 1H), −0.48 (d, J = 13 Hz, 2H), −0.83 (m, 1H), −1.04 (m, 2H), −2.79 (s, 2H), −3.60 (d, J = 11 Hz, 2H), and −4.83 (m, 1H).

X-ray Structure Determinations. All the intensity data were collected using graphite monochromated MoKα (λ = 0.71073 Å) radiation. For the data collection using the Bruker (Siemens) SMART CCD area detector system at the University of Wisconsin, the intensity data nominally covered one and a half hemispheres of reciprocal space. The detector was operated in a 512 × 512 mode and was positioned 5.00 cm from the sample. All the structures were solved by direct methods and refined by full-matrix least-squares on F^2. The data were corrected for absorption by the empirical method. Hydrogen atom positions were initially determined by geometry and were refined using a riding model. Non-hydrogen atoms were refined with anisotropic displacement parameters. Thermal ellipsoids in Figures 1−5 are drawn at 35% probability. Crystallographic and refinement data are collected in Table 1.

(i) (OEP)Os(NO)(OEt). Red prism-shaped crystals were grown from hot ethanol. The intensity data were measured as a series of ø oscillation frames each of 0.4° for 20 s/frame. Coverage of unique data was 93.1%

(23) Cheng, L.; Chen, L.; Chung, H.-S.; Khan, M. A.; Richter-Addo, G. B.; Young, V. G., Jr. *Organometallics* **1998**, *17*, 3853−3864.

complete to 25.00 degrees in θ. Cell parameters were determined from a nonlinear least-squares fit of 6001 peaks in the range $2.21 < \theta < 27.40°$. The first 50 frames were repeated at the end of data collection and yielded 5 peaks showing a variation of −0.13% during the data collection. A total of 10057 data were measured in the range $2.21 < \theta < 28.29°$. A total of 251 parameters were refined against 45 restraints and 3680 data to give wR(F^2) = 0.1477 and S = 1.043 for weights of $w = 1/[\sigma^2(F^2) + (0.0960\ P)^2]$, where $P = [F_o^2 + 2F_c^2]/3$. The final R(F) was 0.0540 for the 2858 observed, [$F > 4\sigma(F)$], data. The molecule sits on the crystallographic center of symmetry. The nitrosyl and ethoxide groups are thus given occupancies of 0.5. One ethyl group, C(17)−C(18), was disordered and modeled in two orientations with occupancies of 0.640(19) and 0.360(19) for the unprimed and primed atoms, respectively. Restraints on the positional parameters of the disordered ethyl atoms and the displacement parameters of N(5) and O(2) were required for the refinement to achieve convergence.

(ii) [(OEP)Os(NO)(H_2O)]BF_4·H_2O. Red prism-shaped crystals were grown from a CH_2Cl_2/heptane solution of [(OEP)Os(NO)(HOC_6H_4F)]BF_4 in air at −20 °C. The intensity data were measured as a series of ø oscillation frames each of 0.2° for 120 s/frame. Coverage of unique data was 92.1% complete to 25.00 degrees in θ. Cell parameters were determined from a nonlinear least-squares fit of 6760 peaks in the range $2.50 < \theta < 28.27°$. The first 50 frames were repeated at the end of data collection and showed no significant decay of the sample during the data collection. A total of 8452 data were measured in the range $1.95 < \theta < 28.28°$. A total of 572 parameters were refined against 844 restraints and 7416 data to give wR(F^2) = 0.1436 and S = 1.074 for weights of $w = 1/[\sigma^2(F^2) + (0.0800\ P)^2 + 10.6268\ P]$. The final R($F$) was 0.0547 for the 6582 observed, [$F > 4\sigma(F)$], data. Although the cation sits in a general position in the unit cell, the anions are split between two different centers of symmetry. Because the anions cannot have inversion symmetry, both anion sites are disordered and are modeled in two orientations. The refined occupancies for the A site atoms are 0.238(8) and 0.262(8) for the unprimed and primed atoms, respectively. The refined occupancies for the B site atoms are 0.187(8) and 0.313(8) for the unprimed and primed atoms, respectively. Restraints to the positional and displacement parameters of the anions were required for the refinement to achieve convergence.

(iii) [(OEP)Os(NO)(HOEt)]BF_4·EtOH. Purple-red crystals were grown from a CH_2Cl_2 solution of (OEP)Os(NO)(OEt) containing HBF_4·Et_2O and ethanol at room temperature. The data were corrected for Lorentz and polarization effects, and an empirical absorption correction based on ψ-scans was applied.[24] The structure was solved by the heavy atom method using the SHELXTL system (Release 5.03) and refined by full-matrix least squares on F^2 using all reflections. Hydrogen atoms were included in the refinement with idealized parameters except for H(1) and H(2) and the hydrogen atoms of the ethanol solvent molecule. H(1) and H(2) were located in the difference map and H(1) was refined isotropically and H(2) was included with fixed positional and thermal parameters (attempts to refine H(2) isotropically were unsuccessful because of the disorder). Other hydrogen atoms belonging to the ethanol solvent molecule could not be located because of the disorder and were not included in the refinement.

The asymmetric unit contains one cation with minor disorder. The overall geometry of the cation is good except for the atoms involved in minor disorder (C(21), C(22), and C(22A)). Both the BF_4 anion and the ethanol solvent molecule are highly disordered, and despite using the SHELXTL restraints of SADI the geometry remained poor, especially for the minor component of the BF_4 anion (F(1A), F(2A), F(3A), and F(4A)) and for the solvent involving C(39A), C(39B), and C(39C) atoms. The ethanol solvent molecule forms a H-bond with the coordinated ethanol as an acceptor, and also with a fluorine atom of the anion as a donor as shown in Figure 3a. Despite the poor geometry of the anion and the solvent molecule, the main objective of this study of establishing the structure of the cation was achieved unambiguously.

(iv) [(OEP)Os(NO)(HOEt/HO^{i}Pr)]BF_4·^{i}PrOH. Red plate-shaped crystals were grown from CH_2Cl_2 solution of (OEP)Os(NO)(OEt) containing HBF_4·Et_2O and 2-propanol at room temperature. The intensity data were measured as a series of ø oscillation frames each of 0.4° for 20 s/frame. Coverage of unique data was 97.3% complete to 25.00 degrees in θ. Cell parameters were determined from a nonlinear least-squares fit of 5713 peaks in the range $2.78 < \theta < 28.27°$. The first 50 frames were repeated at the end of data collection and yielded 289 peaks showing a variation of −0.06% during the data collection. A total of 27987 data were measured in the range $1.80 < \theta < 28.34°$. A total of 535 parameters were refined against 45 restraints and 9772 data to give wR(F^2) = 0.0889 and S = 0.978 for weights of $w = 1/[\sigma^2(F^2) + (0.0470\ P)^2]$. The final R($F$) was 0.0389 for the 7939 observed, [$F > 4\sigma(F)$], data. One ethyl side chain, C(27)−C(28), of the porphyrin ring was disordered and modeled in two orientations with refined occupancies of 0.535(8) and 0.465(8) for the unprimed and primed atoms. The alcohol group chelated to the metal appeared to be two different species, ethanol and 2-propanol. The refined occupancies for the alcohol group were 0.856(6) for ethanol [O(2)−C(38)] and 0.144(6) for 2-propanol [O(2′)-C(39′)]. The crystal structure also contains a 2-propanol solvent site. One methyl of the solvent C(41) was disordered and modeled in two orientations with refined occupancies of 0.53(5) and 0.47(5) for the unprimed and primed atoms. Restraints on the positional parameters and the displacement parameters of the disordered groups were required for the refinement to achieve convergence.

(v) [(OEP)Os(NO)(HO(CH_2)$_5$$CH_3$)]$BF_4$. Red needle-shaped crystals were grown from CH_2Cl_2/hexane at −20 °C. The intensity data were measured as a series of ø oscillation frames each of 0.4° for 30 s/frame. Coverage of unique data was 99.3% complete to 25.00 degrees in θ. Cell parameters were determined from a nonlinear least-squares fit of 7545 peaks in the range $2.46 < \theta < 29.02°$. The first 50 frames were repeated at the end of data collection and yielded 656 peaks showing a variation of 0.29% during the data collection. A total of 20844 data were measured in the range $1.85 < \theta < 29.02°$. A total of 992 parameters were refined against 133 restraints and 16500 data to give wR(F^2) = 0.0827 and S = 1.008 for weights of $w = 1/[\sigma^2(F^2) + (0.0380\ P)^2]$. The final R($F$) was 0.0369 for the 14924 observed, [$F > 4\sigma(F)$], data. There are two formula units per asymmetric unit of the cell. Restraints on the positional parameters of the hexanol and anion were required for the refinement to converge to a chemically reasonable result.

Results and Discussion

We have shown previously that alkyl nitrites (RO−N═O; R = i-C_5H_{11}, n-Bu) add to the (por)Os(CO) compounds (por = TTP, OEP) to give the six-coordinate trans addition nitrosyl alkoxide products (por)Os(NO)(OR).[4,6,8] A similar reaction of ethyl nitrite EtO−N═O to (OEP)Os(CO) in CH_2Cl_2 at room temperature gives, after workup, the new nitrosyl ethoxide complex (OEP)Os(NO)(OEt) in 78% isolated yield as purple-red crystals. This compound is moderately air-stable in the solid-state, showing no signs of decomposition in air after several days. In aerated solution, however, it decomposes slowly to the known bimetallic μ-oxo compound [(OEP)Os(NO)]$_2$(μ-O).[23] The spectroscopic properties of (OEP)Os(NO)(OEt) are consistent with its formulation as such. Thus, its IR spectrum reveals a strong υ_{NO} band at 1759 cm^{-1} (CH_2Cl_2) or 1756 cm^{-1} (KBr), indicating the presence of a terminal nitrosyl ligand. The ^{1}H NMR spectrum also reveals, in addition to peaks due to the porphyrin protons, peaks at −2.65 (quartet) and −3.11 (triplet) ppm due to the axial OCH_2CH_3 ligand. The solid-state molecular structure was obtained from a single-crystal X-ray crystallographic analysis of a suitable crystal of the compound, and is shown in Figure 1a. Selected bond lengths and angles are shown in Table 2.

The Os−N−O moiety is bent with a bond angle of 156.1(17)°, and the Os−N(O) and OsN−O bond lengths are 1.81(2) and 1.33(2) Å, respectively. The Os−N(porphyrin) distances are 2.069(6) and 2.079(6) Å, and fall within the 1.942(35)-2.169(33)

(24) North, A. T. C.; Philips, D. C.; Mathews, F. S. *Acta Crystallogr*. **1968**, *A24*, 351−359.

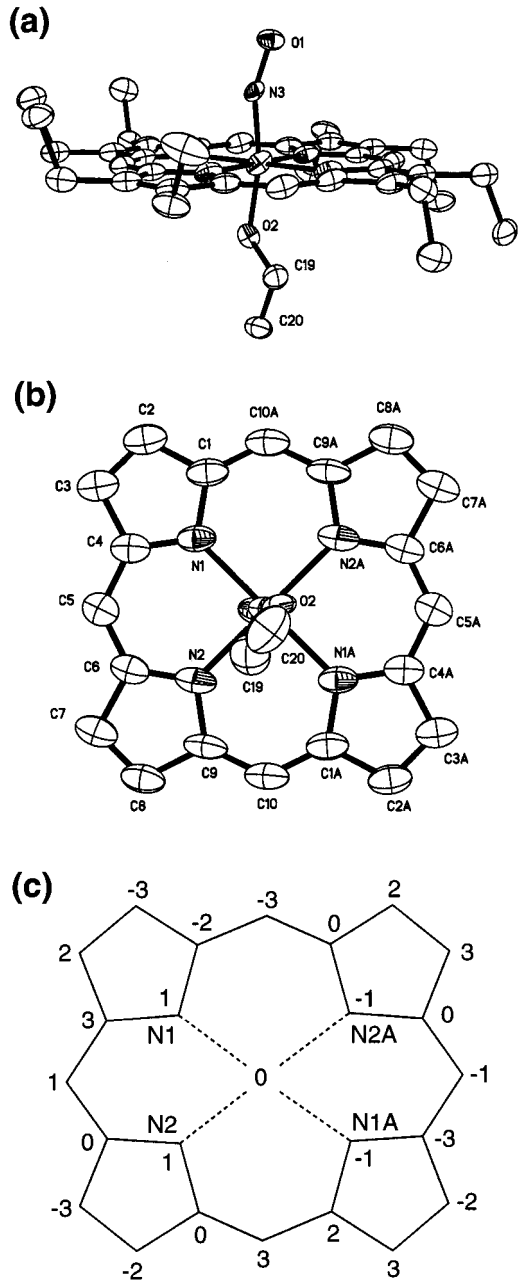

Figure 1. (a) Molecular structure of (OEP)Os(NO)(OEt). Hydrogen atoms have been omitted for clarity. (b) Approximate view along the O(2)−Os bond, showing the orientation of the axial ethoxide group with respect to the porphyrin skeleton. (c) Perpendicular atom displacements from the 24-atom porphyrin plane (in 0.01 Å units). Negative values are displacements toward the porphyrin face containing the NO ligand.

Å range[25] previously observed for other (OEP)Os-containing compounds.[8,25−30] The Os−O(ethoxide) bond length is 1.89(2) Å, and is similar to that seen in (OEP)Os(NO)(O^{n}Bu) (1.877(7) Å) and in the (TPP)Os(OR)$_2$ complexes (R = Et, ^{i}Pr, Ph; 1.909(4)-1.938(2) Å). Other structurally characterized monometallic Os−O(alkoxide) bond lengths fall in the range 1.920(3)-2.200(7) Å.[9−12]

Table 2. Selected Bond Lengths and Angles for (OEP)Os(NO)(OEt)

Bond Lengths (Å)			
Os(1)−N(3)	1.81(2)	Os(1)−N(2)	2.079(6)
N(3)−O(1)	1.33(2)	Os(1)−O(2)	1.89(2)
Os(1)−N(1)	2.069(6)	O(2)−C(19)	1.39(3)
Bond Angles (deg)			
Os(1)−N(3)−O(1)	156.1(17)	N(3)−Os(1)−N(2)	91.9(8)
N(3)−Os(1)−O(2)	167.8(10)	N(3)−Os(1)−N(1)	95.5(8)
Os(1)−O(2)−C(19)	123.7(15)	O(2)−Os(1)−N(2)	95.9(6)
O(2)−Os(1)−N(1)	93.8(6)		

The axial nitrosyl N atom of (OEP)Os(NO)(OEt) is tilted 5.4° from the normal to the 24-atom porphyrin plane, and a tilt of 7.5° is observed for the O atom of the trans ethoxide ligand. The resulting (O)N−Os−O(ethoxide) bond angle is 167.8(10)°. Axial nitrosyl N-atom tilts in porphyrins have been observed in iron,[31−33] cobalt,[34] and ruthenium porphyrins.[33,35] The relative orientation of the ethoxide ligand with respect to the porphyrin core is shown in Figure 1b; the N(2)−Os(1)−O(2)−C(19) torsion angle is 11°. Perpendicular displacements of the 24 atoms of the porphyrin core are shown in Figure 1c.

Preparation of Nitrosyl Alcohol Complexes. Prior to the current study, no alcohol complexes of osmium nitrosyl porphyrins had been reported. Protonation of (OEP)Os(NO)(OEt) with tetrafluoroboric acid in ethanol solvent gives the cationic alcohol complex [(OEP)Os(NO)(HOEt)]$^+$ complex as the tetrafluoroborate salt in 90% isolated yield. The υ_{NO} of the complex occurs at 1828 cm^{-1} (CH_2Cl_2), which is 69 cm^{-1} higher than that of the precursor ethoxide complex, and indicates less Os→NO back-bonding in the cationic ethanol complex. In situ ^{1}H NMR measurements show that protonation of (OEP)Os(NO)(OEt) in $CDCl_3$ also generates the cationic alcohol complex, although we find that protonation in the presence of ethanol solvent allows for the isolation of the complex in high yield, suggesting that perhaps the alcohol ligands do not bind strongly to the [(OEP)Os(NO)]$^+$ fragment. Indeed, in contrast to the neutral ethoxide precursor complex which was moderately air-stable, the cationic product is air-sensitive, giving the new [(OEP)Os(NO)(H_2O)]$^+$ and known [(OEP)Os(NO)]$_2$(μ-O)[23] complexes upon exposure of the cationic ethanol complex to air.

We have taken advantage of the weak binding of the ethanol ligand in [(OEP)Os(NO)(HOEt)]$^+$ to generate other alcohol complexes (eq 1).

$$\text{(OEP)Os(NO)(OEt)} \xrightarrow{H^+} [\text{(OEP)Os(NO)(HOEt)}]^+ \xrightarrow[-\text{EtOH}]{\text{ROH}} [\text{(OEP)Os(NO)(HOR)}]^+ \quad (1)$$

For example, protonation of (OEP)Os(NO)(OEt) in methanol solvent gives, after appropriate workup, the cationic methanol complex [(OEP)Os(NO)(HOMe)]$^+$ in 91% isolated yield. The use of other alcohols in this protonation reaction allows for the

(25) Masuda, H.; Taga, T.; Osaki, K.; Sugimoto, H.; Mori, M. *Bull. Chem. Soc. Jpn.* **1984**, *57*, 2345−2351.
(26) Scheidt, W. R.; Nasri, H. *Inorg. Chem.* **1995**, *34*, 2190−2193.
(27) Nasri, H.; Scheidt, W. R. *Acta Crystallogr.* **1990**, *C46*, 1096−1098.
(28) Che, C.-M.; Lai, T.-F.; Chung, W.-C.; Schaefer, W. P.; Gray, H. B. *Inorg. Chem.* **1987**, *26*, 3907−3911.
(29) Chen, L.; Khan, M. A.; Richter-Addo, G. B.; Young, V. G., Jr.; Powell, D. R. *Inorg. Chem.* **1998**, *37*, 4689−4696.
(30) Salzmann, R.; McMahon, M. T.; Godbout, N.; Sanders, L. K.; Wojdelski, M.; Oldfield, E. *J. Am. Chem. Soc.* **1999**, *121*, 3818−3828.
(31) Scheidt, W. R.; Duval, H. F.; Neal, T. J.; Ellison, M. K. *J. Am. Chem. Soc.* **2000**, *122*, 4651−4659, and references therein.
(32) Ellison, M. K.; Scheidt, W. R. *J. Am. Chem. Soc.* **1997**, *119*, 7404−7405.
(33) Richter-Addo, G. B.; Wheeler, R. A.; Hixson, C. A.; Chen, L.; Khan, M. A.; Ellison, M. K.; Schulz, C. E.; Scheidt, W. R. Manuscript in preparation.
(34) Ellison, M. K.; Scheidt, W. R. *Inorg. Chem.* **1998**, *37*, 382−383.
(35) Hodge, S. J.; Wang, L.-S.; Khan, M. A.; Young, V. G., Jr.; Richter-Addo, G. B. *Chem. Commun.* **1996**, 2283−2284.

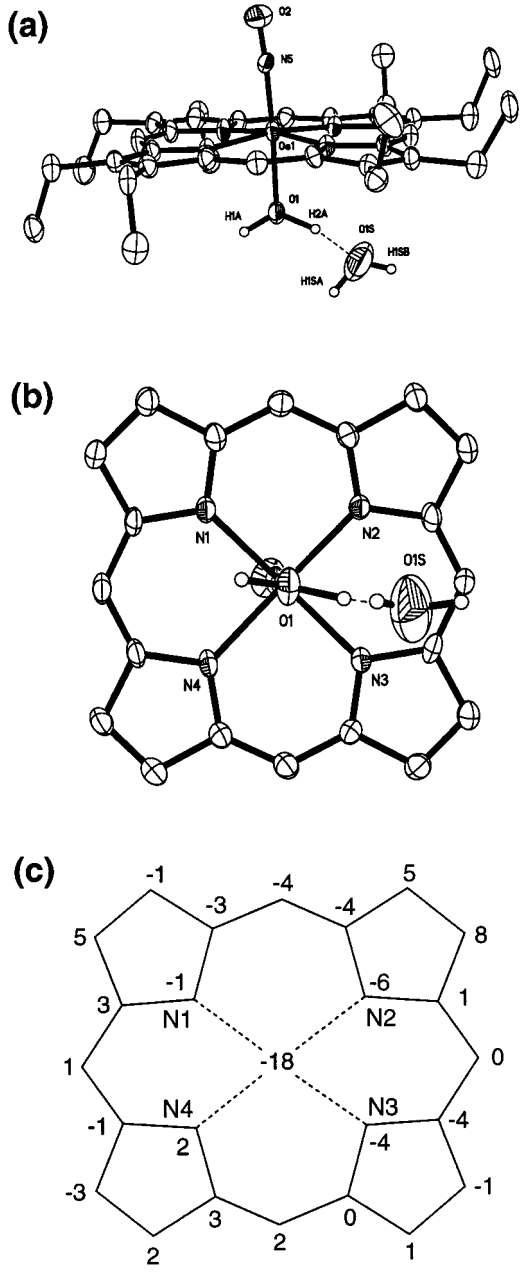

Figure 2. (a) Molecular structure of the cation of [(OEP)Os(NO)(H$_2$O)]BF$_4$·H$_2$O. Most hydrogen atoms have been omitted for clarity. (b) Approximate view along the O(1)−Os bond, showing the orientation of the aquo solvate with respect to the porphyrin skeleton. (c) Perpendicular atom displacements from the 24-atom porphyrin plane (in 0.01 Å units). Negative values are displacements toward the porphyrin face containing the NO ligand.

preparation of their cationic osmium derivatives in high yields for the 2-propanol (96% yield), hexanol (92% yield), and cyclohexanol (92% yield) solvents. The ν_{NO} bands of the aliphatic alcohol [(OEP)Os(NO)(HOR)]$^+$ complexes in CH_2Cl_2 are at 1828 cm^{-1}, or fall in the narrow 1813−1816 cm^{-1} range as KBr pellets. We have not yet been able to isolate a related complex containing a *tertiary* alcohol ligand (e.g., *tert*-butyl alcohol), presumably due to unfavorable steric interactions between the porphyrin macrocycle and the bulky *tert*-butyl group of the alcohol.

We have also been able to prepare an aryl alcohol complex, namely [(OEP)Os(NO)(HOC$_6$H$_4$F)]$^+$, by performing the protonation in heptane in the presence of added 4-fluorophenol. The aryl alcohol ligand is labile, and our attempts to crystallize

Table 3. Selected Bond Lengths and Angles for [(OEP)Os(NO)(H$_2$O)]BF$_4$·H$_2$O

Bond Lengths (Å)			
Os(1)−N(5)	1.726(6)	Os(1)−N(3)	2.061(6)
N(5)−O(2)	1.153(9)	Os(1)−N(4)	2.067(6)
Os(1)−N(1)	2.060(6)	Os(1)−O(1)	2.071(5)
Os(1)−N(2)	2.056(6)	O(1)···O(1S)	2.482(10)
Bond Angles (deg)			
Os(1)−N(5)−O(2)	176.6(6)	N(5)−Os(1)−N(4)	92.4(3)
N(5)−Os(1)−O(1)	176.7(2)	O(1)−Os(1)−N(1)	84.9(2)
N(5)−Os(1)−N(1)	92.0(3)	O(1)−Os(1)−N(2)	84.5(2)
N(5)−Os(1)−N(2)	96.6(3)	O(1)−Os(1)−N(3)	86.6(2)
N(5)−Os(1)−N(3)	96.5(3)	O(1)−Os(1)−N(4)	86.6(2)

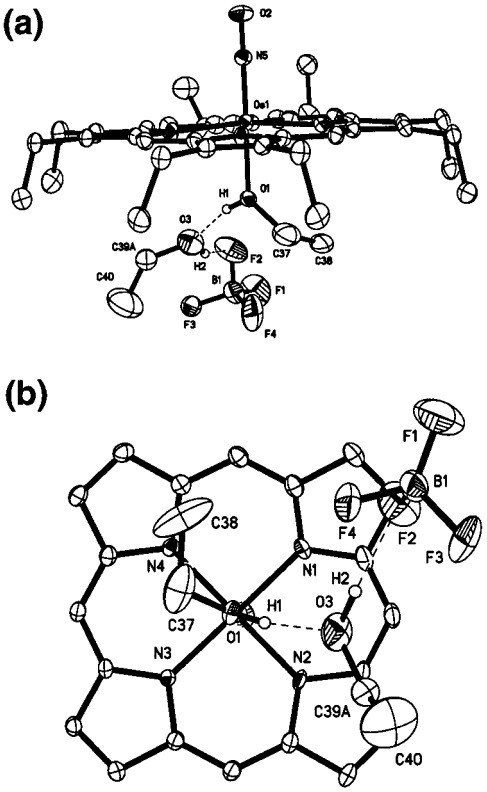

Figure 3. (a) Molecular structure of [(OEP)Os(NO)(HOEt)]BF$_4$·HOEt. Most hydrogen atoms have been omitted for clarity. (b) Approximate view along the O(1)−Os bond, showing the orientation of the axial ethanol group, ethanol solvate, and the anion with respect to the porphyrin skeleton. Distances (Å) and angles (deg): O(1)···O(3) = 2.554(6), O(3)···F(2) = 2.782(12), O(1)−H(1)···O(3) = 165.3, O(3)−H(2)···F(2) = 157.2.

this compound from CH_2Cl_2/heptane in air at −20 °C resulted in the formation of the new [(OEP)Os(NO)(H$_2$O)]$^+$ aqua derivative, presumably from the introduction of moisture during the crystallization process. This aqua derivative was characterized by X-ray crystallography, and the solid-state structure is shown in Figure 2, and selected bond lengths and angles are collected in Table 3.

The Os−N−O group is linear with a bond angle of 176.6(6)°, and the Os−N(O) and N−O distances are 1.726(6) and 1.153(9) Å, respectively. The nitrosyl N-atom is tilted 4.1° away from the normal to the 24-atom mean porphyrin plane, and a smaller tilt of 2.2° is observed for the O-atom of the axial aquo ligand. The complex contains a water solvent molecule (Figure 2a). Although the resulting [(OEP)Os(NO)(H$_2$O)]BF$_4$·H$_2$O complex is stoichiometrically similar to the ruthenium analogue [(OEP)Ru(NO)(H$_2$O)]BF$_4$·H$_2$O previously reported by us,[36] an important difference between the two exists which manifests itself in subsequent chemical reactivity. In the Os complex, the axial

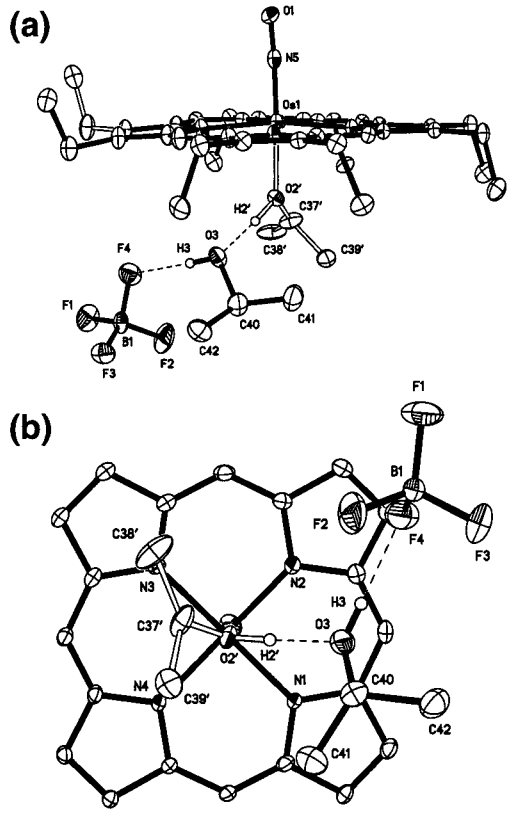

Figure 4. (a) Molecular structure of the $[(OEP)Os(NO)(HO^iPr)]BF_4 \cdot {}^i$PrOH component of $[(OEP)Os(NO)(HOEt)]BF_4 \cdot {}^i$PrOH/$[(OEP)Os(NO)(HO^iPr)]BF_4 \cdot {}^i$PrOH. Most hydrogen atoms have been omitted for clarity. (b) Approximate view along the O(2′)-Os bond, showing the orientation of the axial alcohol group, ^{i}PrOH solvate, and the anion with respect to the porphyrin skeleton. Distances (Å) and angles (deg): O(2)···O(3) = 2.569(4), O(3)···F(4) = 2.702(4), O(2′)−H(2′)···O(3) = 173.2, O(3)−H(3)···F(4) = 178.1

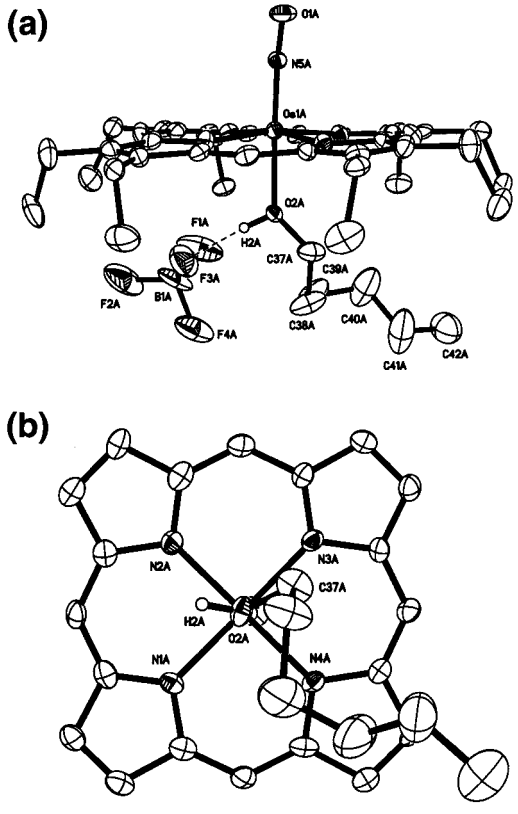

Figure 5. (a) Molecular structure of one form of $[(OEP)Os(NO)(HOhexyl)]BF_4$. Most hydrogen atoms have been omitted for clarity. (b) Approximate view along the O(2A)-Os bond, showing the orientation of the axial alcohol group with respect to the porphyrin skeleton. Distances (Å) and angles (deg): O(2A)···F(3A) = 2.608(7), O(2B)···F(3B) = 2.561(8), O(2A)-H(2A)···F(3A) = 172.7, O(2B)-H(2B)···F(3B) = 176.8

(coordinated) H_2O molecule interacts with the water solvate via a strong hydrogen bond[37] interaction (O(1)···O(1S) = 2.482(10) Å), whereas the equivalent interaction in the Ru analogue is only moderate (3.172(34) Å).[36] The relative orientation of the water molecules in $[(OEP)Os(NO)(H_2O)]BF_4 \cdot H_2O$ is shown in Figure 2b, and the axial displacements of the atoms of the porphyrin core are shown in Figure 2c.

Molecular Structures of Alcohol Complexes. The solid-state structures of the $[(OEP)Os(NO)(HOEt)]^+$, $[(OEP)Os(NO)(HO^iPr)]^+$, and $[(OEP)Os(NO)(HOhexyl)]^+$ compounds are shown in Figures 3, 4, and 5, respectively. For brevity, selected structural parameters are summarized in Figure 6. A common feature in these structures is that the NO and alcohol ligands are situated trans to each other. The nitrosyl ligands are essentially linear (174.4(6)−178.5(3)°), and the axial N(nitrosyl) and O(alcohol) atoms are only very slightly tilted from the normal to the 24-atom mean porphyrin planes, although slightly larger tilts of the N(nitrosyl) atoms are observed in the hexanol complex (3.3−4.6°).

The $[(OEP)Os(NO)(HOEt)]^+$ compound crystallizes as an ethanol solvate (Figure 3). The coordinated EtOH ligand interacts with the ethanol solvate via a moderately strong hydrogen bond[37] (O(1)−O(3) = 2.554(6) Å), and the solvate is also hydrogen bonded to the tetrafluoroborate anion.

In our attempt to obtain crystals of the ^{i}PrOH complex, we obtained suitable X-ray quality crystals from the reaction of $[(OEP)Os(NO)(HOEt)]^+$ with ^{i}PrOH at room temperature. However, solution of the crystal structure revealed a mixture of the $[(OEP)Os(NO)(HOEt)]^+$ and $[(OEP)Os(NO)(^iPrOH)]^+$ cations. The molecular structure of the ^{i}PrOH ligated complex is shown in Figure 4. As with the pure EtOH complex described earlier (Figure 3), the ^{i}PrOH ligand is hydrogen bonded to the ^{i}PrOH solvate via a moderately strong interaction (O(2)−O(3) = 2.569(4) Å), and the solvate is also hydrogen bonded to the tetrafluoroborate anion.

The hexanol complex, on the other hand, was obtained as an unsolvated complex (Figure 5). In this case, the coordinated hexanol ligand is hydrogen bonded directly to the anion, with (ligand)O-to-F(anion) distances of 2.561(8) and 2.608(7) Å for the two independent molecules.

The C_α-atoms of the alcohol ligands are situated between adjacent porphyrin nitrogens. The smallest (por)N−Os−O−C_α(alcohol) torsion angles are 20.8(7)° for the EtOH complex (Figure 3b), 23.2(4)° for the ^{i}PrOH complex (Figure 4b), and 22.9(5) and 20.9(5)° for the two molecules of the hexanol complex (Figure 5b).

Deprotonation Reactions. Given our observation that other 1° and 2° alcohols could substitute the ethanol ligand in $[(OEP)Os(NO)(HOEt)]^+$, we attempted to prepare the cationic $[(OEP)Os(NO)(py)]^+$ complex by substitution of the alcohol ligand(s) with pyridine. We had previously obtained the ruthenium analogue $[(OEP)Ru(NO)(py)]^+$ by such a displacement reaction.[38] We found, however, that addition of pyridine to the cationic $[(OEP)Os(NO)(HOMe)]^+$ complexes resulted in

(36) Chen, L.; Yi, G.-B.; Wang, L.-S.; Dharmawardana, U. R.; Dart, A. C.; Khan, M. A.; Richter-Addo, G. B. *Inorg. Chem.* **1998**, *37*, 4677−4688.

(37) Jeffrey, G. A. *An Introduction to Hydrogen Bonding*; Oxford University Press: New York, 1997; Table 2.1, p 12.

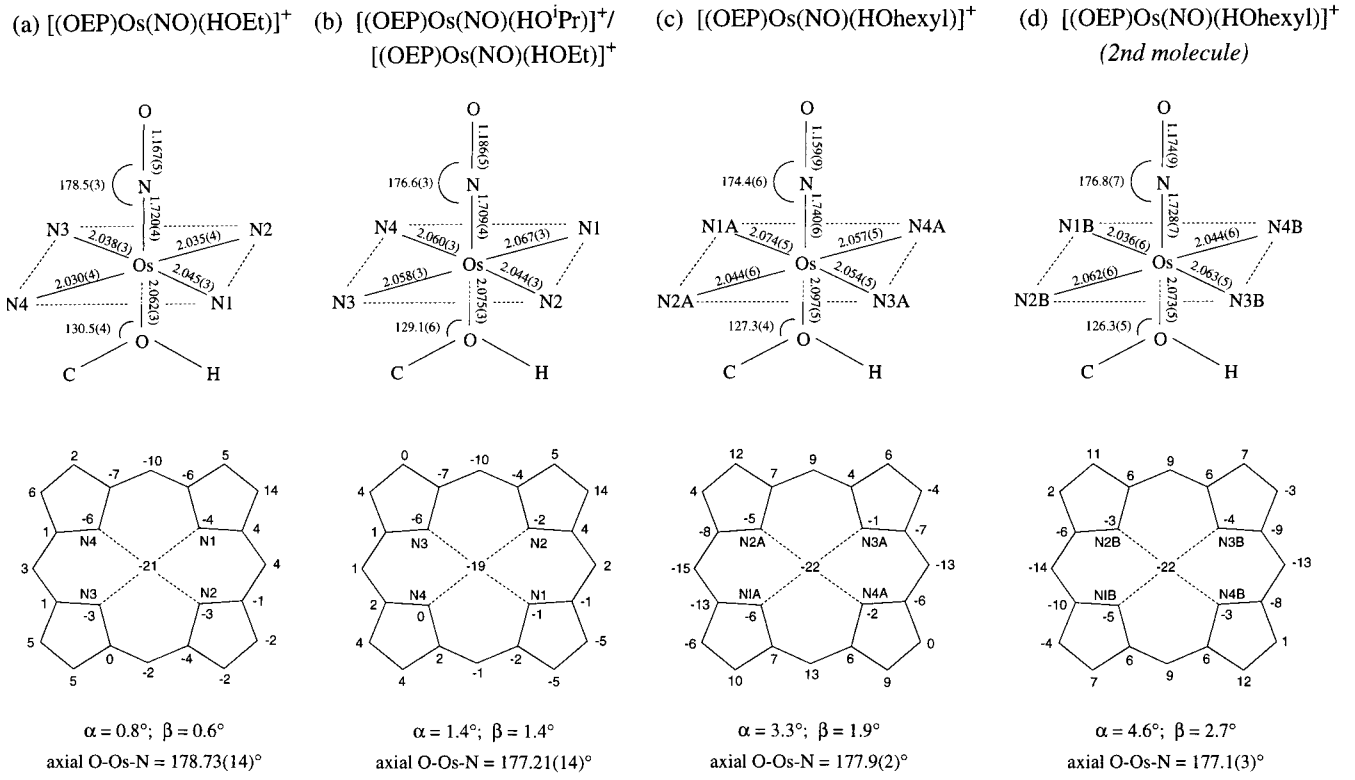

Figure 6. Summary of structural parameters of the [(OEP)Os(NO)(alcohol)]BF_4 compounds shown in Figures 3-5. Alpha (α) refers to the displacement of the axial N(O) atom from the normal to the 24-atom porphyrin plane. Beta (*β*) refers to the analogous displacement of the axial O atom (of the alcohol ligand) from the normal to the 24-atom porphyrin plane. The axial atom displacements (bottom) are shown for the orientations of the porphyrin planes shown in Figures 3c, 4c, and 5c, with the alcohol ligands on the top side of the plane.

deprotonation of the coordinated alcohol to give the neutral alkoxide (OEP)Os(NO)(OMe) derivative in 70% isolated yield. It thus appears that the $[(OEP)Os(NO)]^+$ fragment is sufficiently electrophilic to activate the bound alcohol ligands toward deprotonation. Indeed, the electrophilic nature of $[(OEP)Os(NO)]^+$ is probably responsible for the preferred binding of the negatively charged alkoxide ligands rather than the neutral pyridine ligand. The electrophilic nature of this cation in its BF_4 salt also results in the production of the fluoride (OEP)Os(NO)F compound[23,39] when the deprotonation is carried out under laboratory lighting and/or under longer (>5 min) reaction times. We also observed the conversion of the desired (OEP)Os(NO)(OR) products to the known $[(OEP)Os(NO)]_2(\mu$-O) oxo-dimer[23] if the nitrosyl alkoxides are allowed to remain in contact with the silica gel column for extended periods.

The occurrence of this deprotonation event using pyridine suggested to us that other (OEP)Os(NO)(OR) complexes could then be readily prepared by the corresponding deprotonation reactions of their precursor cationic alcohol complexes. Indeed, this turned out to be the case, and provided an entry into a new convenient route for the syntheses of other (OEP)Os(NO)(OR) complexes. For example, protonation of (OEP)Os(NO)(OEt) in 2-propanol solvent followed by solvent removal gave crude solid $[(OEP)Os(NO)(HO^iPr)]^+$ (eq 2).

$$(OEP)Os(NO)(OEt) \xrightarrow[PrOH]{H^+} [(OEP)Os(NO)(HO^iPr)]^+ + EtOH \quad (2)$$

$$[(OEP)Os(NO)(HO^iPr)]^+ \xrightarrow[-pyH^+]{py} (OEP)Os(NO)(O^iPr) \quad (3)$$

Addition of pyridine to a CH_2Cl_2 solution of this crude $[(OEP)Os(NO)(HO^iPr)]^+$ then generated the neutral (OEP)Os(NO)(O^iPr) derivative in 65% overall isolated yield (eq 3). The hexyl and cyclohexyl alkoxide derivatives were obtained similarly in 60−70% isolated yields.

We note that although the iron porphyrin methoxide complex (TTP)Fe(OMe) reacts with less electron-rich alcohols R′OH to form new (TTP)Fe(OR′) derivatives,[40] the (OEP)Os(NO)(OR) complexes do not appear to react in a similar manner even under refluxing conditions. This is probably due, in part, to the presence of the trans *π*-acid NO ligand which withdraws electron density away from the alkoxide O-atom making the alkoxide ligand less susceptible to attack by acid. Indeed, we have previously observed that the $[(OEP)Os(NO)]_2(\mu$-O) oxo-dimer is unusually unreactive toward acid due to the presence of two trans NO ligands.[23]

Summary. In summary, we have prepared the first alcohol complexes of osmium nitrosyl porphyrins. Their single-crystal X-ray structures represent the first solid-state structures of osmium alcohol complexes to be reported. We have shown that the electrophilic $[(OEP)Os(NO)]^+$ cation in the $[(OEP)Os(NO)(HOR)]^+$ complexes renders the coordinated alcohol ligands susceptible to deprotonation by pyridine, thus generating new (OEP)Os(NO)(OR) derivatives. This latter reaction represents a new and convenient route to the preparation of the alkoxide derivatives of osmium nitrosyl porphyrins.

Acknowledgment. We are grateful to the National Institutes of Health (FIRST Award GM53586) and the National Science

(38) Fomitchev, D. V.; Coppens, P.; Li, T.; Bagley, K. A.; Chen, L.; Richter-Addo, G. B. *Chem. Commun.* **1999**, 2013−2014.
(39) Buchler, J.; Smith, P. D. *Chem. Ber.* **1976**, *109*, 1465−1476.
(40) Shaffer, C. D.; Straub, D. K. *Inorg. Chim. Acta* **1989**, *158*, 167−180.

Foundation (NSF CAREER Award CHE-9625065) for funding for this research. Grants from the NSF and from the University of Wisconsin and the University of Oklahoma for the purchase of the Bruker (Siemens) X-ray diffractometers and computers are also acknowledged.

Supporting Information Available: Drawings and listings of X-ray structural data. This material is available free of charge via the Internet at http://pubs.acs.org.

IC0007512